• Clinical Research •

Safety evaluation after LASIK surgery based on the linear creep property: a finite element analysis

Ji-Xi Guo[1], Xue-Feng Li[1], Xin-Chao Wang[1], Xin-Heng Zhao[2], Yan Wang[2], Li-Hua Fang[1]

[1]Key Laboratory for Optoelectronic Information Perception and Instrumentation of Jiangxi Province, Nanchang Hangkong University, Nanchang 330063, Jiangxi Province, China
[2]Tianjin Key Lab of Ophthalmology and Visual Science, Tianjin Eye Institute, Tianjin Eye Hospital; Nankai University Eye Institute, Nankai University; Clinical College of Ophthalmology, Tianjin Medical University, Tianjin 300000, China
Correspondence to: Li-Hua Fang. Key Laboratory for Optoelectronic Information Perception and Instrumentation of Jiangxi Province, Nanchang Hangkong University, Nanchang 330063, Jiangxi Province, China. fanglh71@126.com
Received: 2024-03-01 Accepted: 2024-10-10

Abstract

● **AIM:** To investigate the effect of the percent tissue altered (PTA) on the safety after laser-assisted *in situ* keratomileusis (LASIK) based on linear creep characteristics.

● **METHODS:** The linear creep characteristics of the cornea were characterized by the generalized Kelvin-Voigt constitutive relationship with five parameters. Then, the displacement and stress distribution on the anterior and posterior surfaces of the cornea were analyzed by constructing the eye model with different PTA.

● **RESULTS:** When PTA was above 39%, the vertex displacements under physiological intraocular pressure (IOP, 15 mm Hg) exceeded that of the preoperative glaucoma under average IOP. That is, an excessively high displacement value was found. In addition, with the increase of PTA, the central cornea was stretched thinner and more obviously due to IOP. When PTA was above 39%, the stress at the center of the anterior surface of the residual stroma was more than 20% larger than that of the normal human eye. The residual stroma was forced to stretch more severely due to excessive stress on the anterior surface. This resulted in deformation of the stroma and induced corneal ectasia. Meanwhile, the postoperative vertex displacement increased with the decrease in viscosity ratio.

● **CONCLUSION:** PTA less than 39% is the safe range for LASIK surgery. This study may provide a reliable numerical basis for postoperative corneal dilatation and the outcomes after refractive surgery.

● **KEYWORDS:** laser-assisted *in situ* keratomileusis; finite element; percent tissue altered; vertex displacement
DOI:10.18240/ijo.2025.05.15

Citation: Guo JX, Li XF, Wang XC, Zhao XH, Wang Y, Fang LH. Safety evaluation after LASIK surgery based on the linear creep property: a finite element analysis. *Int J Ophthalmol* 2025;18(5):889-896

INTRODUCTION

Laser *in situ* keratomileusis (LASIK) has been performed for more than 30y, and much clinical research has supported its predictability, efficiency and safety[1-3]. However, refractive surgery ablated part of the anterior corneal stroma, which threatened the stability and integrity of the cornea. In a few cases, corneal ectasia after LASIK does occur, with a 0.25% to 0.6% incidence. This complication remains a focus of refractive surgery research[4-7]. Previous studies have summarized the causes of corneal ectasia after LASIK, including high myopia, thinner residual stromal thickness (RST), and higher percent tissue altered (PTA)[8-9]. In clinical, PTA is determined by the ratio between the sum of cut thickness and flap thickness, and the preoperative central corneal thickness (CCT). Spadea *et al*[10] and Randleman *et al*[11] believed that thinner RST was the main factor contributing to corneal ectasia. Santhiago *et al*[12] hold that PTA provided a more personalized measure of the risk assessment. Compared to specific RST or CCT preoperatively, PTA considered the relationship between corneal thickness, tissue alteration through ablation and flap creation, and ultimate RST. Moreover, a higher PTA value was more likely to induce corneal ectasia. PTA can be expressed as:

$$PTA=(FT+AD)/CCT \quad (1)$$

where FT: flap thickness, AD: ablation depth[13].

The biomechanical properties of cornea are not only determined by its stable structure, but also by its complex material properties. Cornea tissue is a typical viscoelastic material, and creep is one of its essential properties. Creep refers to the phenomenon that strain increases over time while stress is unchanged[14]. Studies have obtained the stress-strain, stress relaxation, and creep curves of corneal stroma through the uniaxial tensile tests. These were used to research

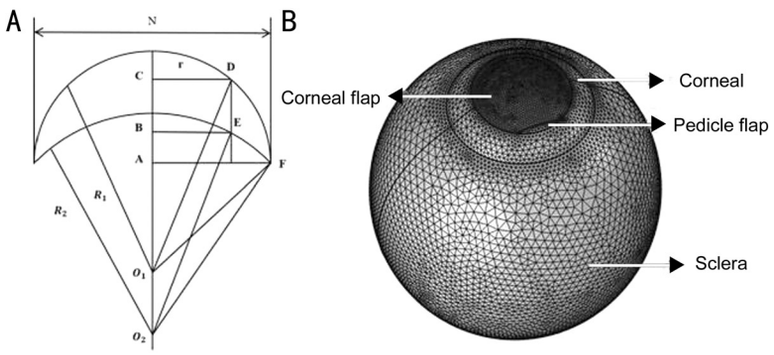

Figure 1 Curvature radius and finite element mesh A: The diagram of corneal anterior surface curvature radius before and after refractive surgery; B: Finite element mesh of the personalized model of the human eye.

the biomechanical properties of the corneal stroma, such as nonlinearity and viscoelasticity[15-16]. Nguyen *et al*[17] deduced the nonlinear anisotropic viscoelastic constitutive model of the corneal stroma, which can well predict and verify the stress-strain and the nonlinear creep behaviors of the corneal strips. Ahmed *et al*[18] studied standard Linear Solid (SLS) model is better describing the human corneal behavior in response to constant and transient load more efficiently.

The finite element method is a computational tool that can be used to represent the geometric, biomechanical, and biological characteristics of a structure. It has been widely used in the research of biomedical engineering in recent years, especially in the analysis of human tissues such as eyeballs, teeth, and bones[19-20]. It is also a valuable tool for comparing the biomechanical properties for various surgical options and providing insight into safety assessments for surgical parameters[21-22].

In this study, the personalized three-dimensional (3D) models for pre and post LASIK was reconstructed. The generalized five-element linear Kelvin-Voigt constitutive equation was used to characterize the corneal creep property. Additionally, the effects of the corneal materials' viscosity ratio on creep results were discussed. The postoperative models for various PTA based on the actual eye model were reconstructed. Finally, the transient dynamic calculation in the finite element model was performed to analyze the displacement and stress distribution on the anterior and posterior surfaces of the cornea with different PTA.

PARTICIPANTS AND METHODS

Ethical Approval The data for this study were obtained from participants at the Tianjin Eye Hospital. The study protocol adhered to the ethical requirements of the Declaration of Helsinki, and the protocol was approved by the Research Ethics Committee of Tianjin Eye Hospital.

Personalized Geometric Model of the Human Eye The geometric parameters were measured by the pentacam rotating scheimpflug camera and the LenStar 900. The CCT was 540 μm, and the curvature radius of the corneal anterior and posterior surfaces were 8.06 mm and 6.66 mm, respectively. The sclera had a horizontal diameter of 26.48 mm and a vertical diameter of 24.48 mm, with an anteroposterior diameter of 27.52 mm. A preoperative geometric model of the subject was reconstructed. The equatorial portion was thin, and the posterior pole was the thickest.

The spherical equivalent (SE) errors are -8.75 diopters (D) and the astigmatic refractive errors was -0.25 D for the subject. The schematic diagram of corneal tissue ablation in refractive surgery was showed in Figure 1A. The ablation profile was expressed by the Munnerlyn equation as follows:

$$h(r) = \sqrt{{R_1}^2 - r^2} - \sqrt{\left(\frac{(n-1)R_1}{n-1+SR_1}\right)^2 - r^2} - \sqrt{{R_1}^2 - \frac{O^2}{4}} + \sqrt{\left(\frac{(n-1)R_1}{n-1+SR_1}\right)^2 - \frac{O^2}{4}} \quad (2)$$

Where O is the diameter of the optical zone in refractive surgery (6 mm), n represents the corneal refractive index with a value of 1.376, and S conveys the diopter of subject with myopia. R_1 indicates the curvature radius of the corneal anterior surface before refractive surgery, and h represents the ablation depth.

The tetrahedral mesh was created by using the physical field division mesh function. The cornea was the primary focus of this study, resulting in a more detailed mesh division. and the number of mesh elements was 179 340. The convergence of the model was verified by analyzing the results of grid calculations with different densities. But it was worth noting the number of mesh elements for the corneal model with different PTA varied slightly. The meshed personalized model of the human eye after surgery was given in Figure 1B. In the figure, the mesh for the cornea is clearly smaller than that for the sclera.

Construction of Creep Constitutive Equation The characterization of material creep properties of materials actually includes two parts: viscosity properties and elastic properties, that is, the material viscoelasticity. In order to improve the accuracy and adaptability of the simulation, a generalized Kelvin-Voigt linear viscoelastic creep model with five parameters was used. In our study, the model was reconstructed by a spring in series with two Kelvin-Voigt models. Through data fitting, it was found that the creep

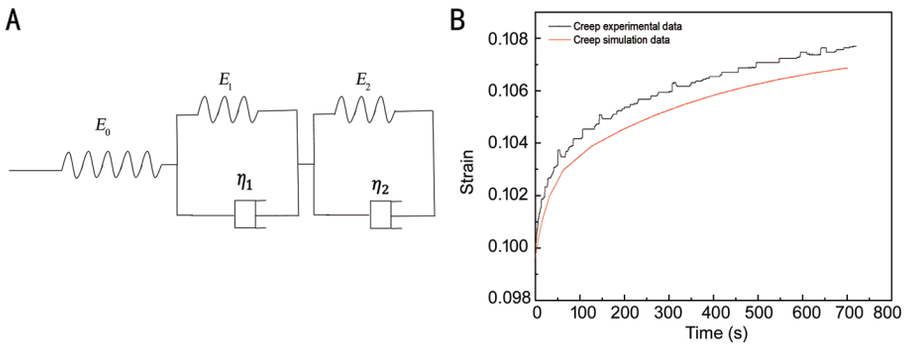

Figure 2 Construction and verification of creep constitutive equation A: Five-element linear viscoelastic Kelvin-Voigt model; B: Comparison of uniaxial tension test and simulation results.

properties of the cornea could be well described. The model diagram was as Figure 2A. The linear viscoelastic constitutive equation of the Kelvin-Voigt model with five elements was described as follows:

$$\varepsilon(t) = \frac{\sigma_0}{E_0} + \frac{\sigma_0}{E_1}\left(1 - \exp\left(-\frac{t}{\tau_1}\right)\right) + \frac{\sigma_0}{E_2}\left(1 - \exp\left(-\frac{t}{\tau_2}\right)\right) \quad (3)$$

Where σ_0 is the initial stress, $E_i(i=0,1,2)$ represents the Young's modulus of the spring, $\eta_i(i=1,2)$ conveys the viscosity coefficient of the dashpot, and

$$\tau_i = \frac{\eta_i}{E_i}(i = 1,2)$$

conveys the relaxation time. The experimental data of uniaxial tension of corneal stroma were used to fit, and the creep equation was obtained as follows:

$$\varepsilon(t) = 0.10026 + \frac{0.0029354}{28.59} \times \exp\left(-\frac{t}{28.59}\right) + \frac{0.0053637}{404.57} \times \exp(-t/404.57) \quad (4)$$

The strip model of corneal stroma was established to simulate the uniaxial tension experiment, and the tension in the creep experiment was set and kept constant. Creep behavior was simulated in the finite element, and the results were compared with actual creep experimental data on fresh human corneal stroma to verify the availability of creep constitutive equations[23]. As demonstrated in Figure 2B, the simulation results showed that the strain values were essentially consistent with those of the creep experiment, and the maximum error was only 0.763%. These results indicated that this creep constitutive equation was appropriate for this study.

Material Properties Table 1 showed the normal material parameters and the intraocular pressure (IOP)[24-25]. The creep constitutive equation was loaded to the cornea in finite element analysis software. The uniform pressure was vertically applied to all inner surfaces of the model to simulate IOP. The fixation constraint had been applied to the sclera at the bottom.

Viscosity generally refers to the ability to resist deformation. Moreover, clinically, there are significant individual differences in viscosity. Therefore, the relationship between corneal viscosity and displacement deserves great attention. According to the generalized Kelvin-Voigt linear viscoelastic creep model with five parameters, a new index of corneal viscosity was defined, *i.e.*, the viscosity ratio. It referred to the ratio of viscosity gradient for different creep test data while the purely elastic strain keeping constantly. Based on the original creep test data, the ratios of viscosity were obtained by adjusting the corresponding strain while the stress maintaining constants. In fact, the viscosity ratio for the original creep test data was set to 1. In this study, the ratio of viscosity being 0.33, 0.5, 0.67, 2 and 3 were used. Table 2 showed the parameters of creep constitutive equation with different viscosity ratios.

Table 1 Material properties

Region	Modulus of elasticity, MPa	Density, kg/m³	Poisson's ratio	IOP, mm Hg
Cornea	1.2	1067	0.499	15
Sclera	2.4	1243	0.499	15

IOP: Intraocular pressure.

Table 2 The parameters of creep constitutive equation with different viscosity ratios

Parameters	The parameters of creep constitutive equation				
Viscosity ratios (σ/ε)	σ_0/E_0	σ_0/E_1	σ_0/E_2	τ_1/s	τ_2/s
0.33	0.099678	0.008319	0.016102	28.137	397.27
0.5	0.099658	0.005546	0.010735	28.137	397.27
0.67	0.099649	0.004159	0.008050	28.137	397.27
1	0.100260	0.002935	0.005364	28.590	404.57
2	0.099630	0.001387	0.002684	28.137	397.27
3	0.099626	0.000924	0.001789	28.137	397.27

σ: Stress; ε: Strain; E: Young's modulus; τ: Relaxation time.

RESULTS

Effect of Corneal Viscosity Ratio on Vertex Displacement

The creep constitutive equations with different viscosity ratios were obtained by data fitting. Figure 3A showed the creep curves for five viscosity ratios. According to Newton's law of viscosity, the viscosity coefficient was inversely proportional to the strain rate when the stress was constant. Therefore, the viscosity ratio decreases as the viscosity gradient increases.

The vertex displacement on the anterior and posterior surfaces of the cornea after refractive surgery under different viscosity ratios was indicated in Figure 3B, with the IOP at 15 mm Hg.

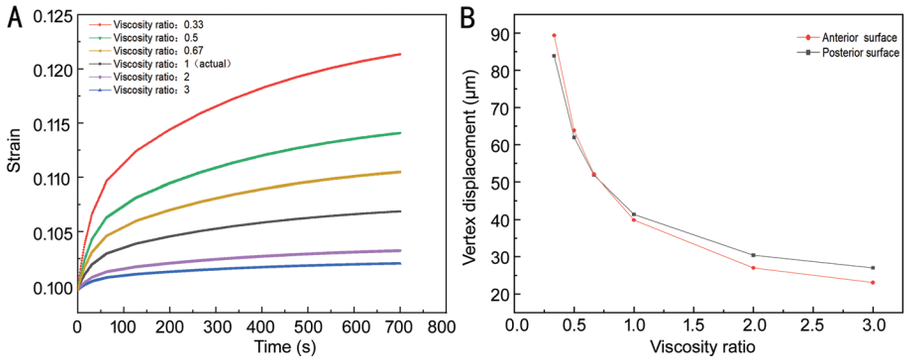

Figure 3 Creep experimental curves and vertex displacement under different viscosity ratios A: Creep experimental curves for different viscosity ratios; B: The vertex displacement of the anterior and posterior surfaces under different viscosity ratios.

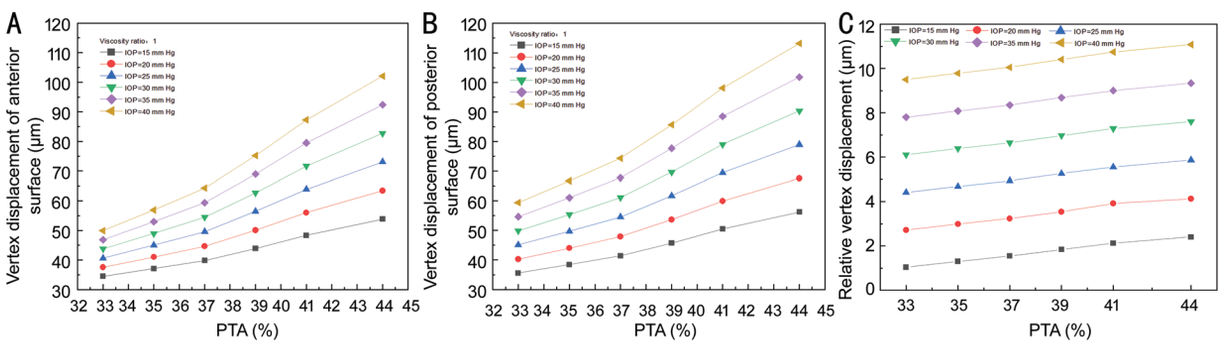

Figure 4 Relationship between IOP and PTA with vertex displacements A: The anterior corneal surface; B: The posterior corneal surface; C: The vertex displacement difference between posterior surface and anterior surface of cornea. IOP: Intraocular pressure; PTA: Percent tissue altered.

The results suggested that the displacement of the anterior and posterior surfaces decreased with the increase in viscosity ratio. When the viscosity ratio was greater than 0.67, the vertex displacement of the posterior surface was always greater than that of the anterior surface. The difference in vertex displacement between the anterior and posterior corneal surfaces increased with the viscosity ratio increasing. But when the viscosity ratio was less than 0.67, the vertex displacement of the posterior surface was smaller than the anterior surface.

Influence of PTA and IOP on Vertex Displacement In fact, the displacement on corneal surfaces was significantly influenced by IOP. Here, the maximum IOP was set to 40 mm Hg, which corresponds to the IOP in glaucoma. On the other hand, clinically, there were significant individual differences in PTA between each refractive surgery. Therefore, it is worthwhile to further study the relationship between IOP and PTA with corneal vertex displacement. Based on the model of the human eye, the postoperative models with different PTA were reconstructed by keeping the corneal flap thickness and the ablation depth unchanged. Specific parameters were shown in Table 3 and the case four corresponded to was the actual human eye. The vertex displacement on the corneal anterior and posterior surfaces for the models in different PTA by loading IOP in the range of 15 to 40 mm Hg was analyzed.

As indicated in Figure 4A and 4B, under the same IOP, the vertex displacement increased nonlinearly with the PTA increase. To investigate the vertex displacement of the posterior surface for different PTA models under physiological IOP (15 mm Hg), that of the preoperative human eye under different IOP was compared with it. The results showed that the vertex displacement for PTA models being 44% under 15 mm Hg was the same as that of the human eye under IOP being 60 mm Hg. When PTA was 39%, the vertex displacement under 15 mm Hg reached the value of that the human eye under IOP being 40 mm Hg. However, when PTA was 33%, the vertex displacement under 15 mm Hg corresponded only to that of the human eye under IOP being 21 mm Hg. Previous studies had shown that IOP of most glaucoma patients was less than 21 mm Hg[26-28]. Another study showed that the average IOP for refractory postpenetrating keratoplasty glaucoma patients was 41 mm Hg[29].

Table 3 Geometric parameters of models under different PTA

Case	FT, μm	AD, μm	CCT, μm	RST, μm	PTA, %
One	90	108	450	252	44
Two	90	108	480	282	41
Three	90	108	510	312	39
Four(actual)	90	108	540	342	37
Five	90	108	570	372	35
Six	90	108	600	402	33

FT: Flap thickness; AD: Ablation depth; CCT: Central corneal thickness; RST: Residual stromal thickness; PTA: Percent tissue altered.

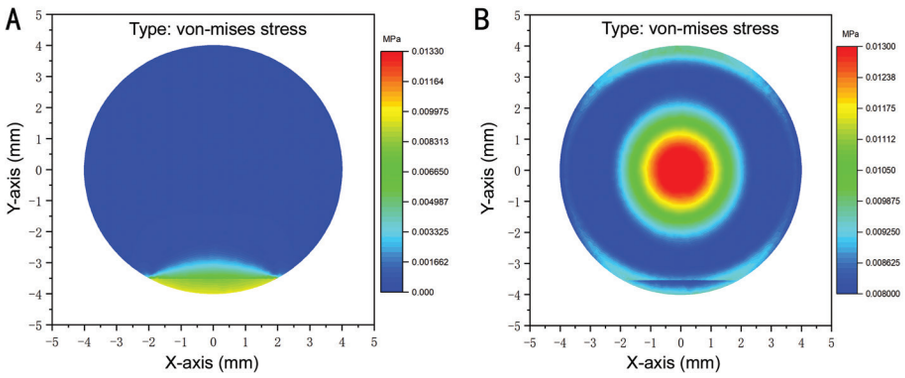

Figure 5 The stress nephogram of the anterior corneal surface after refractive surgery (IOP was 15 mm Hg, PTA was 37%) A: Corneal flap; B: Pedicle flap and the residual stroma. IOP: Intraocular pressure; PTA: Percent tissue altered.

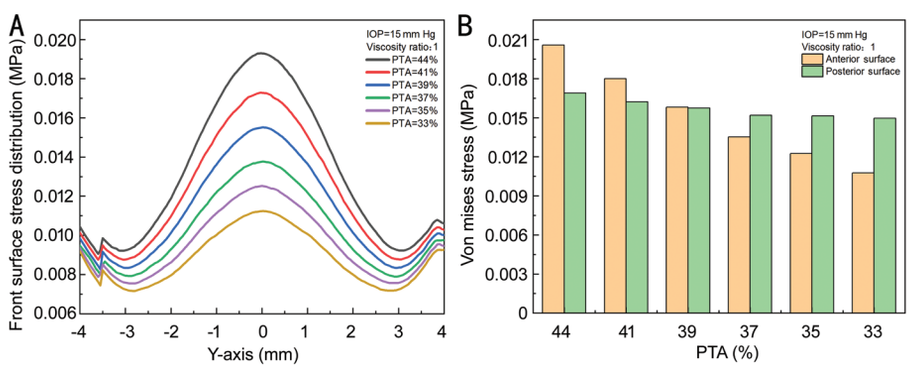

Figure 6 The stress of the corneal surface under different PTA A: Stress distribution curves of anterior surface in Y-axis direction under different PTA; B: The stress in the center of the anterior and posterior surfaces under different PTA. IOP: Intraocular pressure; PTA: Percent tissue altered.

Consequently, when PTA was above 39%, the vertex displacements for the postoperative eye under physiological IOP were higher than that for the refractory postpenetrating keratoplasty glaucoma under the average IOP. It was clear that even under physiological IOP, high PTA certainly resulted in very significant vertex displacement.

In addition, under the same PTA, there was a linear relationship between corneal vertex displacement and IOP. With the increase of PTA, the displacement increased, and the curve became steeper. To reveal the thinning of the cornea, the vertex displacement difference between the anterior and posterior corneal surfaces was calculated. The results indicated that the displacement difference increased with the increase of IOP and PTA in Figure 4C. In the extreme case, when PTA was 44% and IOP was 40 mm Hg, the CCT was reduced by 11.08 μm. The value was about six times larger than that of the eye under physiological IOP.

Effect of PTA on the Stress on Corneal Surface Figure 5 demonstrated the stress distribution on the anterior corneal surface after refractive surgery. As indicated in Figure 5A, there was almost no stress on the corneal flap, while the stress on the pedicle flap was more significant. This was consistent with previous findings[30]. Therefore, the corneal flap was neglected when analyzing the stress on the cornea after refractive surgery. As represented in Figure 5A, the stress on the anterior surface of the residual stroma first decreased and then increased from the edge to the center. The maximum stress occurred in the central corneal zone, about 0.0138 Mpa, which was much larger than the stress of the preoperative cornea in the central zone. The stress on the pedicle flap was only 0.0071 Mpa, which was much smaller than that in the center zone.

Furthermore, the Y-axis stress of the anterior surface of residual stroma under different PTA was analyzed. As demonstrated in Figure 6A, the stress in the Y-axis direction of the anterior surface was regionally distributed. Under the same PTA, the stress tended to be larger in the middle and smaller on both sides. With the PTA increase, the more significant stress concentration in the central area was found. There was a small stress peak at -3.3 mm, caused by the pedicle flap. Additionally, there was a small stress peak at 3.8 mm, caused by the incision at the edge of the flap. Overall, the stress increased with the PTA increase.

Meanwhile, the stress in the center of the anterior and posterior surfaces of the residual stroma was extracted under different PTA with loading the physiological IOP. The effect of PTA on postoperative biomechanics was analyzed quantitatively. As demonstrated in Figure 6B, the stress in the center on the

anterior surface decreases nonlinearly with the decrease of PTA, but the stress on the posterior surface varied little with the decrease of PTA. When PTA was above 39%, the stress in the center on the posterior surface was smaller than that of the anterior surface. However, when PTA was below 39%, the stress on the posterior surface was larger than that on the anterior surface. In addition, when PTA was 39%, the stress in the center on the anterior and posterior surfaces was essentially equivalent.

DISCUSSION

In this study, a generalized five-element linear Kelvin-Voigt model was used to characterize the corneal creep property. The accuracy and adaptability of the constitutive equation were confirmed by the simulation of the uniaxial tensile test. When IOP remained a constant, the lower ratio of viscosity was corresponded to the lower corneal resistance to deformation, resulting in greater corneal vertex displacement. It indicated that the viscosity had a significant influence on corneal deformation after refractive surgery. Figure 7 showed the difference in corneal vertex displacement with or without creep characteristics. Consequently, corneal viscosity is an important consideration before LASIK refractive surgery for candidate patients.

Santhiago *et al*[13] reported that the PTA being lager 40% was the most significant variable associated with the development of corneal ectasia. In this study, creep characteristic was used for finite element analysis under different PTA. The results showed that the stress on the corneal surface tended to be larger in the central zone but smaller in peripheral zone after refractive surgery. With the PTA increase, the stress concentration in the central region was more obvious, and the stress on the corneal surface increased. However, the stress on the posterior surface varied little. Under the same IOP, the vertex displacement increased nonlinearly with the PTA increase. When PTA was greater than 39%, the tensile resistance of the remaining interstitial tissue becomes lower as more corneal tissue was ablated. An increase in the stress in local zone on the anterior surface of the remained corneal stroma was found, and excessive stress may cause change in the fibrous structure within the corneal stroma. The deformed fibrous structure, in turn, induced the stress concentration being more pronounced. This trend manifested macroscopically as corneal lordosis, and thinning. This may intensify the occurrence of postoperative corneal dilatation. It has been reported that the anterior 40% of the corneal stroma has higher tensile strength than the posterior 60%. The tensile strength decreased with the increased depth in the corneal stroma[11,31]. Because the portion of the corneal stroma with maximum stiffness was ablated after refractive surgery, the cornea in the central zone may be stretched thinner, more pronouncedly with

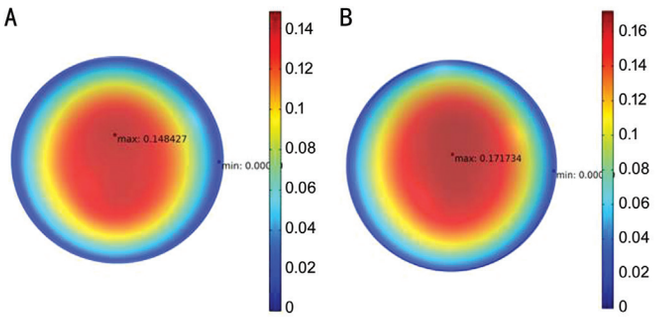

Figure 7 The distribution map of corneal displacement A: The distribution map of corneal displacement without creep characteristics; B: The distribution map of corneal displacement with creep characteristics.

the increase of PTA under IOP. This may increase the risk of corneal ectasia after refractive surgery.

Finite element analysis is not only commonly utilized in the study of the pathogenesis of various eye diseases but also the simulation of clinical operation. Early scholars used finite element method to quantitatively analyze the reduction of the mechanical properties of the tissue after LASIK surgery[32]. The findings suggested that flap-based procedures produced a 49% (range: 2% to 87%) greater mean reduction in effective stromal collagen fiber stiffness within the flap region than contralateral small incision lenticule extraction (SMILE) cases. Another study suggested that both SMILE and LASIK surgery procedures changed the postoperative corneal biomechanics, but LASIK had greater impact on the biomechanics of corneal[33]. These results indicated that LASIK had a higher risk of corneal dilation than SMILE. Dupps *et al*[34] conducted the large-scale 3-dimensional structural analysis of the ectasia risk and PTA was used in an analysis of risk variables. This indirectly indicated that the importance of PTA in evaluating the safety during refractive surgery. Nevertheless, the changes in highly sensitive factors such as PTA and IOP were ignored and the overall model structure was relatively simplistic.

Some clinical studies had conducted statistical analysis on patients with corneal dilation after refractive surgery. The scholars had analyzed the influence of PTA on the efficacy, safety, predictability and stability in post-LASIK ectasia risk assessment[35]. The findings suggested that PTA was not exclusive to determine post-LASIK ectasia risk. But preoperative PTA calculation was of great help in myopia and astigmatism refractive correction. Another recent study suggested that some preoperative risk factors for corneal ectasia had been identified, including abnormal corneal topography, low RST, relatively young patient age, low preoperative corneal thickness, PTA≥0.4[36]. Currently, the calculation method of PTA for different refractive surgeries is different. Undeniably, PTA is still a highly reliable metric for preoperative refractive surgery planning[37].

However, this study has certain limitations. Eye data of a subject with SE of -8.75 D was used as the basis for the model. The 77 types of finite element models were constructed. Although a large number of subjects would enhance the research content, in reality, there were significant individual differences in the human eye. This resulted in significant differences in postoperative models and material parameters. Therefore, although the study of a single human eye had its limitations, it may reduce the impact of individual differences and don't actually significantly affect the results observed in this study. Additionally, the lens, ciliary body, and aqueous humor were not reconstructed in our human eye model based on linear creep characteristics, in order to ensure computational efficiency and simulation accuracy. Their influence on corneal biomechanical response may be hardly affect the accuracy of our study's results. This study explored the influence of IOP and PTA on corneal vertex displacement, finding that under the same IOP, vertex displacement increased nonlinearly with PTA. Due to the subject's high myopia, this fact may have different results to a emmetropic or hyperopic eye model in high IOP conditions. Studies had shown that IOP and refractive power will affect the postoperative visual quality[38]. Consequently, the comprehensive influence of PTA, refractive power, IOP on the safety of refractive surgery is worthy of further study.

In conclusion, the corneal deformation and stress distribution under different PTA with creep characteristics were analyzed based on the finite element method, and the influence of different PTA on the biomechanical properties of the cornea after LASIK refractive surgery was discussed. The results indicated that the postoperative vertex displacement decreased with increasing the corneal ratio of viscosity. The vertex displacement and stress increased with PTA increasing, and the anterior surface was more susceptible to be influenced than the posterior surface. When PTA was above 39%, the vertex displacements for the postoperative eye under physiological IOP were significantly higher than that for the glaucoma under the average IOP. In addition, the stress on the anterior surface of the residual stroma was significantly increased. These may lead to corneal dilation after refractive surgery. Therefore, PTA less than 39% is the safe range for LASIK surgery. This study may provide a reliable numerical basis for postoperative corneal dilatation and the outcomes after refractive surgery.

ACKNOWLEDGEMENTS

Authors' Contributions: All authors contributed to the study conception and design. The overall content and ideas of the paper are in the charge of Wang Y and Fang LH. Material preparation, data collection and analysis were performed by Guo JX, Li XF and Zhao XH. The software help was provided by Wang XC. The first draft of the manuscript was written by Guo JX and Li XF. All authors commented on previous versions of the manuscript and approved the final manuscript.

Foundations: Supported by National Natural Science Foundation of China (No.62165010); The National Key Research and Development Program of China (No.2022YFC2404502).

Conflicts of Interest: Guo JX, None; **Li XF,** None; **Wang XC,** None; **Zhao XH,** None; **Wang Y,** None; **Fang LH,** None.

REFERENCES

1 Pallikaris IG, Papatzanaki ME, Stathi EZ, *et al*. Laser *in situ* keratomileusis. *Lasers Surg Med* 1990;10(5):463-468.

2 Tülü Aygün B, Çankaya Kİ, Ağca A, *et al*. Five-year outcomes of small-incision lenticule extraction vs femtosecond laser-assisted laser *in situ* keratomileusis: a contralateral eye study. *J Cataract Refract Surg* 2020;46(3):403-409.

3 Zhang G, Cao H, Qu C. Efficacy, safety, predictability, and stability of LASIK for presbyopia correction: a systematic review and meta-analysis. *J Refract Surg* 2023;39(9):627-638.

4 Moshirfar M, Tukan AN, Bundogji N, *et al*. Ectasia after corneal refractive surgery: a systematic review. *Ophthalmol Ther* 2021;10(4):753-776.

5 Lei YL, Hou J, Zheng XY. Redo surgery using IntraLase femtosecond laser for treating a decentered laser *in situ* keratomileusis flap. *J Int Med Res* 2018;46(2):901-907.

6 Sahay P, Bafna RK, Reddy JC, *et al*. Complications of laser-assisted *in situ* keratomileusis. *Indian J Ophthalmol* 2021;69(7):1658-1669.

7 Zhao LT, Yin YW, Hu T, *et al*. Comprehensive management of post-LASIK ectasia: from prevention to treatment. *Acta Ophthalmol* 2023;101(5):485-503.

8 Jin SX, Dackowski E, Chuck RS. Risk factors for postlaser refractive surgery corneal ectasia. *Curr Opin Ophthalmol* 2020;31(4):288-292.

9 El-Naggar MT, Elkitkat RS, Ziada HE, *et al*. Assessment of preoperative risk factors for post-LASIK ectasia development. *Clin Ophthalmol* 2023;17:3705-3715.

10 Spadea L, Cantera E, Cortes M, *et al*. Corneal ectasia after myopic laser *in situ* keratomileusis: a long-term study. *Clin Ophthalmol* 2012;6:1801-1813.

11 Randleman JB, Dawson DG, Grossniklaus HE, *et al*. Depth-dependent cohesive tensile strength in human donor corneas: implications for refractive surgery. *J Refract Surg* 2008;24(1):S85-S89.

12 Santhiago MR, Smadja D, Wilson SE, *et al*. Role of percent tissue altered on ectasia after LASIK in eyes with suspicious topography. *J Refract Surg* 2015;31(4):258-265.

13 Santhiago MR, Smadja D, Gomes BF, Mello GR, Monteiro ML, Wilson SE, Randleman JB. Association between the percent tissue altered and post–laser in situ keratomileusis ectasia in eyes with normal preoperative topography. *Am J Ophthalmol* 2014;158(1):87-95.

14 Song D, Lim S, Park J, *et al*. Linear viscoelasticity of human sclera and posterior ocular tissues during tensile creep. *J Biomech* 2023;151:111530.

15 Mahdian M, Seifzadeh A, Mokhtarian A, *et al*. Characterization of the transient mechanical properties of human cornea tissue using the tensile test simulation. *Mater Today Commun* 2021;26:102122.

16 Ávila FJ, del Barco Ó, Marcellán MC, *et al*. A comprehensive study on elasticity and viscosity in biomechanics and optical properties of the living human cornea. *Photonics* 2024;11(6):524.

17 Nguyen TD, Jones RE, Boyce BL. A nonlinear anisotropic viscoelastic model for the tensile behavior of the corneal stroma. *J Biomech Eng* 2008;130(4):041020.

18 Ahmed HM, Salem NM, Al-Atabany W. Human cornea thermo-viscoelastic behavior modelling using standard linear solid model. *BMC Ophthalmol* 2023;23(1):250.

19 Babaei B, Shouha P, Birman V, *et al*. The effect of dental restoration geometry and material properties on biomechanical behaviour of a treated molar tooth: a 3D finite element analysis. *J Mech Behav Biomed Mater* 2022;125:104892.

20 Zhang QL, Chon T, Zhang Y, *et al*. Finite element analysis of the lumbar spine in adolescent idiopathic scoliosis subjected to different loads. *Comput Biol Med* 2021;136:104745.

21 Sun XT, Zhang Y, Mei XK, *et al*. Changes in posterior corneal elevation after small incision lenticule extraction for different myopic diopters. *Int J Ophthalmol* 2024;17(3):491-498.

22 Wang CY, Li XN, Guo Y, *et al*. Effects of laser *In situ* keratomileusis and small-incision lenticule extraction on corneal biomechanical behavior: a finite element analysis. *Front Bioeng Biotechnol* 2022;10:855367.

23 Xue C, Xiang YQ, Wang Y, *et al*. Biomechanical properties of normal human corneal stroma. *Recent Advances in Ophthalmology* 2019;39(11):5.

24 Ma JN, Wang Y, Wei PH, *et al*. Biomechanics and structure of the cornea: implications and association with corneal disorders. *Surv Ophthalmol* 2018;63(6):851-861.

25 Fang LH, Ma WW, Wang Y, *et al*. Theoretical analysis of wave-front aberrations induced from conventional laser refractive surgery in a biomechanical finite element model. *Invest Ophthalmol Vis Sci* 2020;61(5):34.

26 Iwase A, Suzuki Y, Araie M, *et al*. The prevalence of primary open-angle glaucoma in Japanese: the Tajimi Study. *Ophthalmology* 2004;111(9):1641-1648.

27 Fujiwara K, Yasuda M, Jun HT, *et al*. Prevalence of glaucoma and its systemic risk factors in a general Japanese population: the hisayama study. *Transl Vis Sci Technol* 2022;11(11):11.

28 Stein JD, Khawaja AP, Weizer JS. Glaucoma in adults-screening, diagnosis, and management: a review. *JAMA* 2021;325(2):164-174.

29 Ates H, Palamar M, Yagci A, *et al*. Evaluation of Ex-PRESS mini glaucoma shunt implantation in refractory postpenetrating keratoplasty glaucoma. *J Glaucoma* 2010;19(8):556-560.

30 Bao FJ, Wang JJ, Cao S, *et al*. Development and clinical verification of numerical simulation for laser *in situ* keratomileusis. *J Mech Behav Biomed Mater* 2018;83:126-134.

31 Randleman JB, Woodward M, Lynn MJ, *et al*. Risk assessment for ectasia after corneal refractive surgery. *Ophthalmology* 2008;115(1): 37-50.

32 Seven I, Vahdati A, Pedersen IB, *et al*. Contralateral eye comparison of SMILE and flap-based corneal refractive surgery: computational analysis of biomechanical impact. *J Refract Surg* 2017;33(7):444-453.

33 Francis M, Khamar P, Shetty R, *et al*. *In vivo* prediction of air-puff induced corneal deformation using LASIK, SMILE, and PRK finite element simulations. *Invest Ophthalmol Vis Sci* 2018;59(13):5320-5328.

34 Dupps WJ Jr, Seven I. A large-scale computational analysis of corneal structural response and ectasia risk in myopic laser refractive surgery. *Trans Am Ophthalmol Soc* 2016;114:T1.

35 Rocha-de-Lossada C, Sánchez-González JM, Rachwani-Anil R, *et al*. Could the percent tissue altered (PTA) index be considered as a unique factor in ectasia risk assessment? *Int Ophthalmol* 2020;40(12):3285-3294.

36 Bohac M, Biscevic A, Ahmedbegovic-Pjano M, *et al*. Management of post-LASIK ectasia. *Mater Sociomed* 2023;35(1):73-78.

37 Smadja D, Mimouni M, Shoshani A, *et al*. Accuracy of the preoperative predicted percentage of tissue altered calculation in refractive surgery planning for myopic LASIK. *J Refract Surg* 2022;38(7):422-427.

38 Du RR, Fang LH, Song YY, *et al*. Effects of intraocular pressure and aspheric transition zone ablation profile on corneal biomechanics after conventional refractive surgery. *E3S Web Conf* 2021;271:03040.